Biochemical and Physical Properties of Remnant-HDL_2 and of Preβ_1-HDL Produced by Hepatic Lipase[†]

Karim Guendouzi,[‡] Beatrice Jaspard,[‡] Ronald Barbaras,[‡] Claude Motta,[§] Claude Vieu,[‡] Yves Marcel,[||] Hugues Chap,[‡] Bertrand Perret,[‡] and Xavier Collet*,[‡]

Institut National de la Santé et de la Recherche Médicale, Unité 326, Phospholipides membranaires, Signalisation cellulaire et Lipoprotéines, Hopital Purpan, 31059, Toulouse Cedex, France, Laboratoire de biochimie, Hotel Dieu, Clermont Ferrand, France, and Lipoprotein and atherosclerosis group, University of Ottawa heart Institute, Ottawa Civic Hospital, Ottawa, Ontario, Canada

Received June 25, 1998; Revised Manuscript Received November 16, 1998

ABSTRACT: The hepatic lipase acting on triglyceride-rich high-density lipoprotein$_2$ (HDL_2) induces the formation of preβ_1-HDL, leaving a residual alpha-migrating HDL particle that was named "remnant-HDL_2" (Barrans, A., Collet, X., Barbaras, R., Jaspard, B., Manent, J., Vieu, C., Chap, H., and Perret, B. (1994) *J. Biol. Chem. 269*, 11572−11577.]. In this study, these two product particles generated by hepatic lipase were isolated by density gradient ultracentrifugation. Particles were first characterized in terms of chemical composition, density, and mass. The preβ_1-HDL obtained in vitro contain one to two molecules of apoA-I, associated with phospholipids, and free and esterified cholesterol. When compared to triglyceride-rich HDL_2, remnant-HDL_2 have lost on average one molecule of apoA-I, 60% of triacylglycerols, and 15% of phospholipids. The estimated composition is concordant with the hypothesis of the splitting of a substrate particle into one preβ_1-HDL and one remnant-HDL_2. Spectroscopic studies were carried out to monitor changes in lipid fluidity upon lipolysis. The fluorescence anisotropy was measured using (1,6)-diphenyl-hexa-(1,3,5)-triene as a probe, and the degree of order was calculated from electron spin resonance spectra using the 5-nitroxy-derivative of stearic acid. Both approaches showed a decreased lipid fluidity in remnant-HDL_2, as compared to triglyceride-rich HDL_2. The immunoreactivity of apoA-I toward several monoclonal antibodies was assayed as a reflection of changes of apoA-I conformation. In remnant-HDL_2, as compared to triglyceride-rich HDL_2, a lower reactivity was noted with the 2G11 antibody, which interacts in the NH_2 terminal part of apoA-I. Finally, remnant-HDL_2 was clearly different from HDL_3 with respect to all of the parameters studied, demonstrating that hepatic lipase does not promote the direct conversion of HDL_2 to HDL_3. Thus, hepatic lipase produces remnant-HDL_2 particles, which display modifications of apoA-I conformation and of fluidity of the lipid environment. This newly described HDL_2 subfraction may play a major role in the reverse cholesterol transport.

The role of HDL[1] in reverse cholesterol transport is closely associated with the interconversion of HDL particles in the vascular compartment. The maturation of small HDL to larger HDL results from the transfer of free cholesterol from the cell membranes to HDL, its esterification by LCAT, and modifications by CETP (*2*, *3*). The backward conversion of HDL_2 to small HDL involves the action of hepatic lipase (HL) (*4*). This interconversion requires the hydrolysis of particle phospholipids and triacylglycerols, associated with the loss of cholesterol, and at least of one molecule of apoA-I per particle (*5*). All of these observations highlight the complex remodeling of HDL particles during their intravascular transit and demonstrate the great plasticity which must be a major feature of apoA-I, allowing it to maintain its association with the highly diverse configurations and compositions of HDL particles (for a review on apoA-I structure, see ref *6*).

The hepatic lipase plays a major role in the HDL remodeling. Earlier studies from our group led us to suggest a model of HDL particles interconversion (*1*). Large HDL particles acquire triacylglycerols from triglyceride-rich lipoproteins in exchange for cholesteryl esters, through the activity of the cholesterol ester transfer protein (CETP) (*7*−*9*). Those large triglyceride-rich HDL_2 then become a preferential substrate for hepatic lipase (*7*, *8*, *10*). In liver perfusion experiments, as well as in vitro, we have demonstrated that hepatic lipase acting on those particles induced the formation of preβ_1-HDL (*1*). This interconversion process results from the reduction of the lipid core of the TG-rich

[†]This work was supported in part by a research grant from ARCOL.

* Correspondence: Xavier Collet, Ph D., Institut National de la Santé et de la Recherche Médicale, Unité 326, Phospholipides membranaires, Signalisation cellulaire et Lipoprotéines, Hôpital Purpan, 31059, Toulouse, France. Tel.: 33 561 77 94 15. Fax: 33 561 77 94 01. E-mail: Collet@cict.fr.

[‡] Hopital Purpan.

[§] Hotel Dieu.

[||] Ottawa Civic Hospital.

[1] Abbreviations: apoA-I, apolipoprotein A-I; CE, cholesteryl ester; DG, diacylglycerol; DPH, 1-6-diphenyl-1,3,5-hexatriene; ESR, electron spin resonance; FA, fluorescence anisotropy; FC, free cholesterol; HDL, high-density lipoprotein(s); HL, hepatic lipase; PL, phospholipid; TG, triacylglycerol; CETP, cholesteryl ester transfer protein; LCAT, lecithin− cholesterol acyl transferase.

10.1021/bi9815086 CCC: $18.00
Published on Web 02/09/1999

HDL$_2$ during lipolysis, leading to the release of excess surface material from the shrinking particle. In this process, apoA-I associated with lipids is released, leaving residual α-migrating particles that we called "remnant-HDL$_2$". Preβ_1-HDL were demonstrated to be the earliest and preferential acceptors of cellular cholesterol, which is then channelled through preβ_2- and preβ_3-HDL, and is further recovered with spherical alpha-HDL (*11*). Several studies have reported the biochemical composition of preβ_1-HDL isolated from plasma (*12*−*15*), and we performed a detailed characterization of the preβ_1-HDL in the extravascular ovarian follicular fluid (*16*). On the opposite, no data are yet available as regards the structure and metabolic fate of the remnant-HDL$_2$ particles, generated through hepatic lipase-mediated lipolysis. Surprisingly, in our liver perfusion experiments, we observed a rapid disappearance of those remnant-HDL$_2$ whereas the preβ_1-HDL accumulated in the medium (*1*). This prompted us to initiate the isolation and the characterization of those particles, together with that of the preβ_1-HDL generated in vitro through the action of hepatic lipase.

Those particles were characterized in terms of size, density, molecular composition, lipid fluidity, and apoA-I conformation.

EXPERIMENTAL PROCEDURES

Materials. Fatty acid-free bovine serum albumin, leupeptin, pepstatin, trasylol, ortho 1,10-phenantrolin, egg yolk lysophosphatidylcholine, and triolein were from Sigma (La Verpillère, France). Heparin was from Choay (Paris, France). Tri[^{3}H]oleoylglycerol- and goat [^{125}I]-labeled anti mouse IgG F(ab′)2 were obtained from Amersham (Les Ulis, France). Monoclonal antibodies against human apoA-I were kindly provided by Dr. Ross Milne and Dr. Yves Marcel (Ottawa, ON, Canada). 1,6-Diphenyl-1,3,5-hexatriene (DHP) was purchased from Fluka (La Verpillère, France) and the ESR probes, 16-doxyl-stearic acid (16-NS) and 5-doxyl-stearic acid (5-NS), were from Sigma.

Lipoprotein Isolation and Modification. Lipoproteins were separated as previously described (*17*) and HDL$_2$ were isolated in the *d*: 1.085−*d*: 1.125 g/mL density interval. After dialysis against Tris/NaCl (10 mM/135 mM), HDL$_2$ (0.2 mM total cholesterol) were enriched in triacylglycerol in the presence of VLDL (0.145 mM free cholesterol), of the $d > 1.21$ g/mL plasma fraction (25% of total volume), as a source of CETP, co-incubated during 6 h at 37 °C (*10*) in the presence of 5,5′-dithio-bis (2-nitrobenzoic acid) (DTNB) as LCAT activity inhibitor. After removing VLDL at 1.07 g/mL, modified HDL$_2$ were reisolated by ultracentrifugation at *d*: 1.21 g/mL, and were further dialyzed against Tris/NaCl (10 mM/135 mM), pH 7.4. TG-rich HDL$_2$ (300 μg/mL of protein) were then incubated with or without HL (80 milliunits/mL) during 2 h at 37 °C in the presence of fatty acid-free albumin. Control TG-rich HDL$_2$ and remnant-HDL$_2$ were reisolated by ultracentrifugation at *d*: 1.21 g/mL. Preβ_1-HDL were obtained at the density *d*: 1.25 g/mL.

Electrophoresis and Transfers. Electrophoresis was run on 0.75% (w/v) Agarose-L (Pharmacia, St Quentin-en-Yvelines, France) in 50 mM barbital buffer (pH 8.6) using GelBond membranes as a support (Pharmacia, Broma, Sweden). After agarose electrophoresis, the gels were then used for passive transfer using distilled water onto 0.45 μm nitrocellulose membranes (Biorad, France). Occasionally, lipoproteins were separated by polyacrylamide gradient gel electrophoresis (4−30%) (Pharmacia). Electrotransfer (Bio-block, Illkirch, France) was carried out in 25 mM Tris-glycine buffer (pH 8.3), containing 20% (v/v) methanol, for 18 h at 30 V and then 1 h at 40 V. All of the electrophoresis and transfers were performed at 4 °C using a Haake FK10 recirculating bath.

Immunoblots. Nitrocellulose blots were incubated for 30 min in 10 mM Tris/HCl, pH 7.4, containing 50 mM NaCl, (buffer A) containing 5% (w/v) skimmed milk. After incubation for 2 h with the mixture of five anti human apoA-I mAbs (4H1 diluted to 1/100 000; 5F6, 5G6, 4F7, and 3G10 diluted to 1/30 000), membranes were washed three times for 30 min with buffer A supplemented with 0.05% (v/v) Tween-20 (buffer B), and were subsequently incubated for 2 h with goat ^{125}I-labeled F(ab′)$_2$ directed against mouse IgG (10^6 cpm/mL). Membranes were washed three times with buffer B. All the incubations were performed at room temperature. Membranes were exposed overnight to a Phosphorimager screen (Molecular Dynamics, France), and the cassettes were imaged by Phosphorimager. Quantitation of apoA-I was performed using ImageQuant 1.0, and data were expressed as pixel points determined by the computer and were linearly correlated with dpm of the ^{125}I bound to the antigen−antibody complex.

Spectroscopic Studies, Fluorescence Polarization, and Electron Spin Resonance. Fluorescence Polarization. Labeling of the lipoprotein particles with (1,6)-diphenyl-(1,3,5)-hexatriene was performed as previously described (*18*). Previous experiments using Trinitrobenzene sulfonic acid as a quencher revealed that over 90% of the probe was incorporated in the HDL envelope (*19*) and that diffusion was negligible.

Electron Spin Resonance. Spin labeling of the lipoprotein particles with the nitroxy-derivatives of stearic acid (5-NS and 16-NS) was performed as previously described (*18*, *20*), using a probe-to-phospholipids ratio of 1:1000. The order parameter was determined from the 5-NS spectra obtained on an ECS 106 Bruker electron spin resonance spectrometer.

Antibodies and Competitive Radioimmunoassays. The antibodies used here have been obtained from mice immunized with either apoA-I or HDL (*21*). Solid-phase radioimmunoassays in the absence of Tween 20 were carried out as described earlier (*22*). Briefly, Remova-wells were coated overnight at 4 °C with 100 μL of 2 μg/mL apo-HDL diluted in a sodium carbonate buffer, pH 7.2. Coated wells were then washed and saturated with 300 μL of PBS containing 0.5% gelatin, for 1 h. Serial dilutions of the samples were prepared in duplicate, and 100 μL of diluted antibodies was added. One hundred microliters of the mix was transferred to the coated wells and then incubated for 1 h. Wells were then washed three times with PBS (pH 7.2) containing 0.05% Tween 20 and incubated with 100 μL of ^{125}I mouse anti-IgG, diluted to 200 000 cpm/μL in the dilution buffer. Wells were washed, blotted dry, and counted in an LKB gamma counter. All of the incubations were performed at room temperature. The dilutions for antibodies 2G11, 3G10, 5F6, A03, A05, A16, and A51 were 1/2000, 1/2800, 1/10 000, 1/800, 1/800, 1/4000, and 1/1000, respectively. Immunoreactivity of the different HDL particles toward mAb was expessed as ED$_{50}$ which is the apoA-I

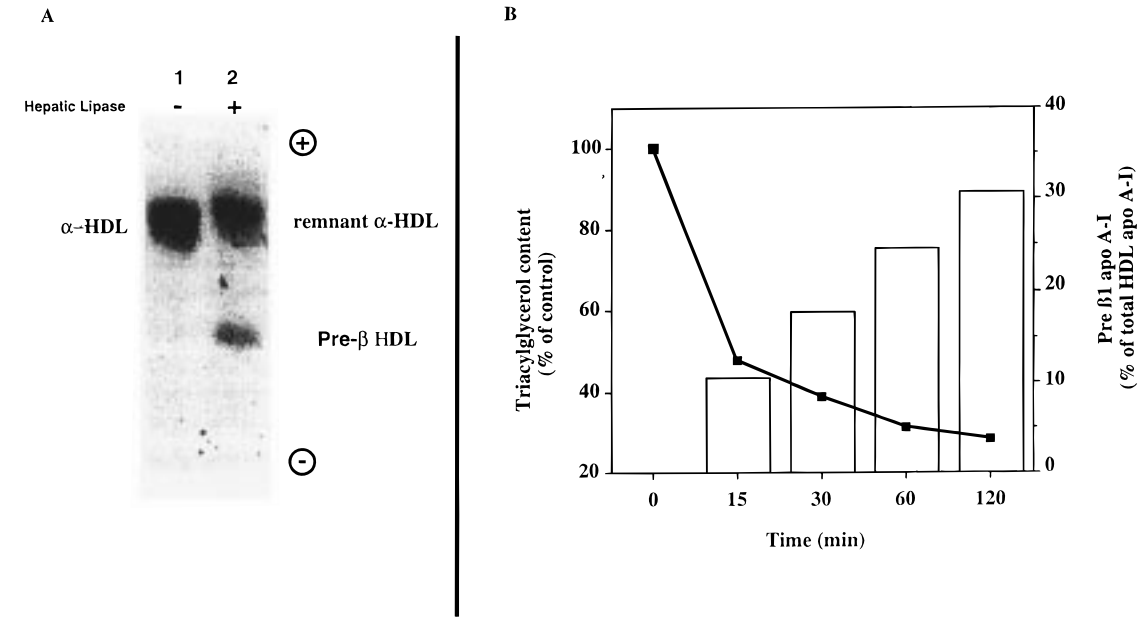

FIGURE 1: (A) Distribution of apo A-I in the post-lipolysis particles (preβ_1-HDL and remnant-HDL$_2$) formed upon incubation of triglyceride-rich HDL$_2$ with hepatic lipase. TG-rich HDL$_2$ (TG-HDL$_2$) were incubated for 120 min at 37 °C in the presence of human HL (80 milliunits/mL) and incubation media were submitted to agarose electrophoresis. Gels were transferred to nitrocellulose and blotted against apo A−I as described in Experimental Procedures. One experiment is representative of three. (B) Kinetics of triacylglycerol hydrolysis of TG-HDL$_2$ (■) and of the appearance of the preβ_1-HDL (columns) during incubation with hepatic lipase. Triacylglycerols and apo A-I were quantified by gas liquid chromatography and immunoelectrodiffusion, respectively, after 0, 15, 30, 60, and 120 min of incubation with hepatic lipase.

concentration inhibiting 50% of the mAb binding onto coated apo HDL.

Miscellaneous. Partial purification of HL from human post-heparin plasma was achieved by heparin affinity chromatography as described previously (*5*). Hepatic lipase activity was assayed according to Nilsson-Ehle and Schotz (*23*), using [^{3}H] triolein as a substrate in the presence of 1 M NaCl. The enzymatic activity expressed as milliunits per milliliter (nanomoles of free fatty acid released per minute per milliliter).

Analytical Procedures. Proteins were measured using the Biorad protein assay dye. Unesterified cholesterol was determined enzymatically (*24*), using commercial kits (Boehringer, Mannheim, F.R.G.). Following lipid extraction, phospholipids were estimated as the lipid phosphorus according to Bottcher et al. (*25*). Phospholipids were separated using the solvent system of Skipski et al. (*26*). Individual spots were scraped off and analyzed as above, to determine the level of phosphatidylcholine hydrolysis. Equilibium density gradient ultracentrifugation (*d*: 1.050 g/mL to *d*: 1.21 g/mL) was performed as reported in ref *5*. Neutral lipid molecular species were quantified by gas−liquid chromatography (GLC) as previously described (*27*).

RESULTS

Formation and Isolation of the Particles Formed by Action of Hepatic Lipase. Triacylglycerol-rich HDL$_2$ (300 μg/mL of protein) were incubated, during 2 h at 37 °C, with or without partially purified human HL (80 milliunits/mL) in the presence of fatty acid-free albumin. After incubation, TG-rich HDL$_2$, treated (Figure 1A, line 2) or not (Figure 1A, line 1), were immediately analyzed by agarose gel electrophoresis. The formation of preβ_1-HDL under the action of HL was evident on the anti apoA-I immunoblots (Figure 1A). The proportion of apoA-I in preβ_1-HDL, as assessed by phosphorimager quantification, was 29.7 ± 4.8% (n = 3). The time course of the appearance of preβ_1-HDL was then followed (Figure 1B). No preβ_1-HDL was detected when triglyceride-rich HDL$_2$ were incubated in the absence of HL. After only 15 min of incubation of triglyceride-rich HDL$_2$ with hepatic lipase, 50% of the triacylglycerol molecules have been hydrolyzed and 10% of apoA-I were recovered in the preβ_1-HDL particles. For longer periods, the formation of preβ_1-HDL was progressively enhanced with the incubation time in the presence of hepatic lipase, while triacylglycerol hydrolysis still increased.

TG-rich HDL$_2$, treated or not by HL, were reisolated by equilibrium density gradient ultracentrifugation. Seventeen 0.7 mL fractions were collected from the top of the tube and were monitored for density, 280 nm O.D, and apoA-I measurements. Based on the distribution of apoAI, control TG-rich HDL$_2$ sedimented as a symmetrical peak, with an average hydrated density of 1.117 ± 0.004 g/mL (n = 3) (Figure 2A). In the case of hepatic lipase-treated TG-rich HDL$_2$, this major peak was shifted by one fraction, giving an average density of 1.124 ± 0.004 g/mL (n = 3). Interestingly, apoA-I was also detected as a minor peak at the highest densities of *d*: 1.20−*d*: 1.22 g/mL, and those fractions corresponded to the preβ_1-HDL, as assessed by polyacrylamide gradient (4−30%) gel electrophoresis. Noteworthy is that the OD A280 and apoA-I distributions fitted exactly, except for the peaks corresponding to the highest densities owing to the presence of bovine serum albumin added in the incubation medium. Particle size was assessed by polyacrylamide gradient gel electrophoresis (4−30%). When individual fractions of gradient ultracentrifugation were analyzed, a homogeneous shift toward smaller sizes was observed (Figure 2B, compare 8 and 9′ and 9 and 10′). Moreover, apoA-I was also present in the heaviest fractions of HL-treated samples only with a band of about 60 kDa, in

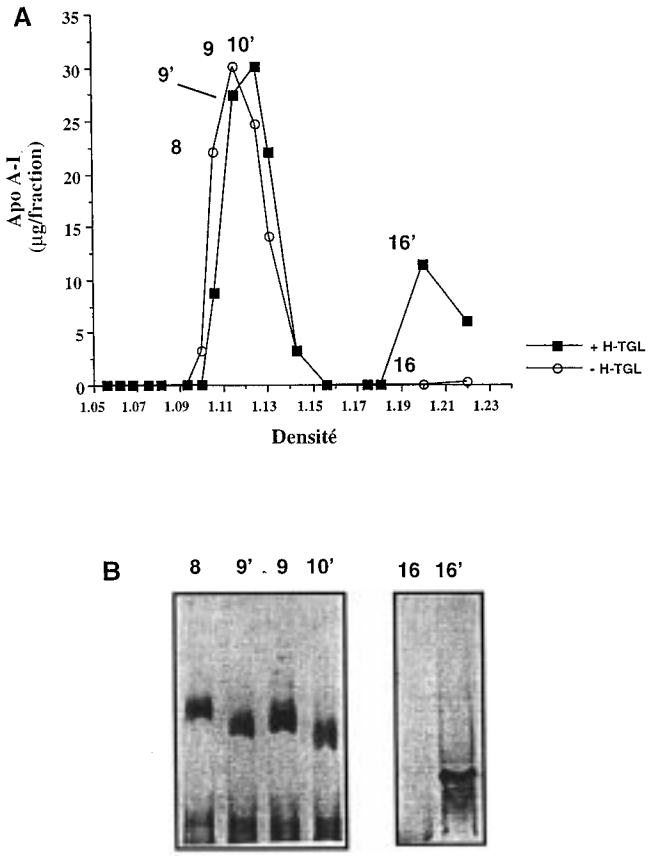

FIGURE 2: (A) Density distribution of apo A-I after equilibrium gradient sedimentation of TG-rich HDL$_2$ treated or not by hepatic lipase (■ and ○, respectively). Density was measured by refractometry and apo A-I was quantified as in Figure 1. (B) Polyacrylamide gradient gel electrophoresis (4−30%) and immunoblot against apo A-I of the fractions containing apo A-I. Numbers 8, 9, and 16 and 9′, 10′, and 16′ refer to the fraction numbers for TG-rich HDL$_2$ and r-HDL$_2$, respectively. One experiment is representative of three.

good agreement with the expected size of preβ_1-HDL (*16*). When HDL particles were reisolated as a pool at *d*: 1.21 g/mL (Figure 3), triglyceride-rich HDL$_2$ displayed a higher molecular mass (327 kDa) than HDL$_2$ (222 kDa) and HDL$_3$ (165 kDa). Upon incubation with hepatic lipase, TG-rich HDL$_2$ were split into preβ_1-HDL (60 kDa) and lipolysed HDL$_2$ (274 kDa) that we will be further referred to as remnant-HDL$_2$.

Biochemical Characterization of the Particles Generated by Hepatic Lipase. The fractions containing apoA-I in the equilibrium density gradient ultracentrifugation were pooled and the lipids were analyzed. Alternatively, remnant-HDL$_2$ were isolated by a single spin at *d*: 1.21 g/mL and preβ_1-HDL were then separated in the *d*: 1.21 and *d*: 1.25 g/mL interval. The profiles of neutral lipid molecular species of the HDL particles were obtained by gas liquid chromatography, according to the total carbon number (Cn) for free cholesterol, diacylglycerols, esterified cholesterol, and triacylglycerols (not shown). All data on lipids were expressed as μmol/mg of apoA-I (Table 1). Incubation of TG-rich-HDL$_2$ with HL induced an average triacylglycerol hydrolysis of 70%. The diacylglycerols remaining in remnant-HDL$_2$ represented 70−130% of the diacylglycerols found in untreated TG-rich-HDL$_2$ (not shown). The amounts of free and esterified cholesterol, as calculated per apoA-I, were not significantly different between control TG-rich-HDL$_2$ and

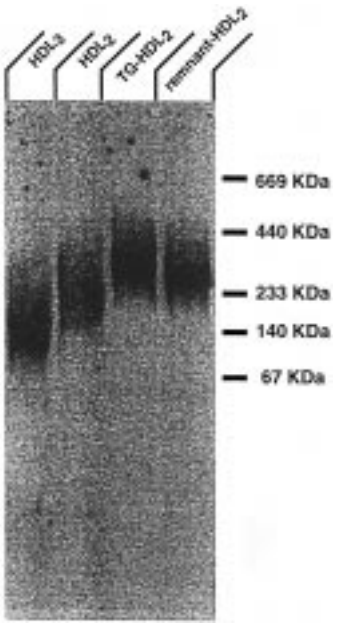

FIGURE 3: Determination of the apparent molecular masses of HDL$_3$, HDL$_2$, TG-rich HDL$_2$, and r-HDL$_2$. All HDL subfractions were reisolated at the density of 1.21 g/mL. The apparent molecular masses were determined by equlibrium polyacrylamide gradient gel electrophoresis (4−30% acrylamide), in the presence of molecular weight standards, followed by an immunoblot against apo A-I, as described in Experimental Procedures.

remnant-HDL$_2$. Free cholesterol represented about 30% of total cholesterol in both cases. The molar ratio of free cholesterol to phospholipids was 0.44 ± 0.10 in remnant-HDL$_2$ compared to 0.38 ± 0.06 in TG-rich HDL$_2$, reflecting the phospholipase A1 activity of HL. The proportion of TG in the lipid core of the particles (TG/TG+CE) was 11.5 ± 2.2% in remnant-HDL$_2$ versus 25.8 ± 2.5% ($p < 0.001$) in TG-rich HDL$_2$, due to the hydrolysis of TG by HL. On the basis of the apoA-I and lipid measurements, and considering the particle masses estimated by gradient gel electrophoresis, the predicted molecular compositions of TG-rich HDL$_2$, remnant-HDL$_2$, and preβ_1-HDL were calculated (Table 2). Hepatic lipase induces the splitting of TG-rich HDL$_2$ into preβ_1-HDL and remnant-HDL$_2$, the latter having lost, on average, one molecule of apoA-I per particle, 16 of phospholipids, and 7 of cholesteryl ester. The reisolated preβ_1-HDL contained 11 molecules of phospholipids, 3 of free cholesterol, 6 of esterified cholesterol, and 1 to 2 apoA-I molecules per particle. Recovery of HDL components after hepatic lipase treatment was quantitative (99%) among remnant-HDL$_2$ and preβ_1-HDL, except for triacylglycerol (−60%) and PL (−5%), which reflects their hydrolysis during incubation.

Physical Properties: Spectroscopic Studies. To monitor changes in the physical properties of HDL following incubation with hepatic lipase, particles were analysed by fluorescence polarization of incorporated diphenyl-hexatriene, and by electron spin resonance using the 5-NS and 16-NS labels. The DPH probe reports the bulk fluidity of the HDL envelope in the condition used, while the 5-NS spectra gives information on the degree of order of the envelope. The parameters were determined at both 24 and 37 °C. The results on lipid dynamics and order parameters are presented in Table 3. The fluorescence anisotropy values of remnant-HDL$_2$ were significantly higher than those of TG-rich HDL$_2$ at both

Table 1: Lipid Composition of the TG-Rich HDL_2 and of the Lipolysis Products Obtained under the Action of Hepatic Lipase[a]

	FC/A-I (μmol/mg)	CE/A-I (μmol/mg)	TG/A-I (μmol/mg)	PL/A-I (μmol/mg)	FC/PL (μmol/mg)	TG/TG + CE (%)
TG-HDL_2 ($n = 9$)	0.34 ± 0.04	0.92 ± 0.11	0.31 ± 0.04	0.99 ± 0.18	0.38 ± 0.06	25.80 ± 2.50
r-HDL_2 ($n = 9$)	0.40 ± 0.07	0.91 ± 0.13	0.12 ± 0.03^b	0.93 ± 0.18	0.44 ± 0.10	11.47 ± 2.17^b
preβ_1-HDL ($n = 4$)	0.046 ± 0.017^c	0.093 ± 0.03	0.02 ± 0.01^d	0.24 ± 0.07^d	0.21 ± 0.03	14.63 ± 6.50

[a] TG-rich HDL_2, remnant-HDL_2 (r-HDL_2), and preβ_1-HDL were reisolated as described in Experimental Procedures. Neutral lipids were analyzed by gas liquid chromatography and apo A-I was quantified by immunoelectrodiffusion. The abbreviations are FC, free cholesterol; CE, cholesteryl esters; PL, phospholipids; TG, triacylglycerols; and DG, diacylglycerols. Results are expressed as means ±SE. Statistical comparisons between TG-rich HDL_2 and r-HDL_2 or preβ_1-HDL were performed using the Student's t test: [b] $p < 0.02$. [c] $p < 0.01$. [d] $p < 0.005$.

Table 2: Molecular Compositions of TG-Rich HDL_2, of Remnant-HDL_2 (r-HDL_2), and of preβ_1-HDL Obtained Following Hepatic Lipase Hydrolysis[a]

molecules/particle	apo A-I	PL	FC	CE	TG	DG
TG-HDL_2 ($n = 3$)	4.72 ± 0.46	100.60 ± 3.94	36.75 ± 5.39	90.64 ± 6.73	50.89 ± 2.41	42.50 ± 7.10
r-HDL_2 ($n = 3$)	3.90 ± 0.55	83.85 ± 4.21	35.13 ± 6.30	83.68 ± 8.40	21.79 ± 5.63	42.92 ± 10.85
preβ_1-HDL ($n = 5$)	1.59 ± 0.14	11.55 ± 2.50	2.76 ± 0.58	5.69 ± 2.56	1.18 ± 0.54	1.69 ± 0.50

[a] Compositions are given as the number of molecules per particle and were calculated from the apparent molecular masses of TG-rich HDL_2 (327 KDa), r-HDL_2 (274 KDa), and preβ_1-HDL (60 KDa) (Figure 3). Abbreviations: PL, phospholipids; FC, free cholesterol; CE, cholesteryl esters; TG, triacylglycerols; DG, diacylglycerols; TG-HDL_2, TG-rich HDL_2; r-HDL_2, remnant HDL_2.

Table 3: Physical Properties of TG-Rich HDL_2 and Remnant-HDL_2 Surface[a]

	fluorescence anisotropy (r)		degree of order (S)	
	24 °C	37 °C	24 °C	37 °C
TG-HDL_2 ($n = 7$)	0.205 ± 0.005	0.170 ± 0.006	0.695 ± 0.015	0.599 ± 0.014
r-HDL_2 ($n = 7$)	0.231 ± 0.008^b	0.189 ± 0.009^b	0.756 ± 0.018^b	0.645 ± 0.026^c

[a] Lipid dynamics (FA) and order parameters were obtained respectively by fluorescence polarization and ESR. HDL were labeled with the lipophilic probe 1,6-diphenyl-1,3,5-hexatriene (DPH) at 24 and 37 °C at a probe/phospholipid molar ratio less than 1/1000 for fluorescence anisotropy. The degree of order was obtained using HDL labeled with 5-NS, at a probe to a phospholipid molar ratio less than 1/1000. The incubation was controlled in order to limit the probe diffusion into the lipoprotein core. [b] Statistical comparison between TG-rich HDL_2 and r-HDL_2: $p < 0.01$. [c] Statistical comparison between TG-rich HDL_2 and r-HDL_2: $p < 0.02$.

temperatures (0.231 vs 0.205 at 24 °C, and 0.189 vs 0.170 at 37 °C). As well, the degree of order was significantly enhanced in remnant-HDL_2 when compared to TG-rich HDL_2. All of these changes reflect a decreased lipid fluidity of the particles envelope following lipolysis. Moreover, the loss of fluidity of the particle core after treatment by the HL was confirmed by ESR using the 16-NS probe (not shown). There was a negative correlation between, on one hand, the triacylglycerol content of the hydrophobic core of the HDL particle, and on the other hand, the fluorescence anisotropy ($r = -0.826$, $n = 18$, Figure 4), as well as the degree of order (S) ($r = -0.855$, $n = 18$, not shown).

ApoAI Immunoreactivity. Competition immunoassays with specific monoclonal antibodies (mAbs) were performed as a means to follow changes in the apoA-I conformation occurring upon lipolysis. The immunoreactivities were compared for TG-rich HDL_2, for remnant-HDL_2, and for HDL_2 and HDL_3, taken as reference of HDL subfractions. All assays were performed in parallel with similar dilutions of apoA-I in the various particles, assayed as competing antigens. Fifteen antibodies, mapping defined epitopes all along the apoA-I structure, were tested, and Table 4 summarizes the data for 7 of them. The ED_{50} values toward the different antibodies varied by more than 1000-fold, reflecting great differences in the exposures of the corresponding epitopes at the surface of HDL. Particles were especially reactive with the 3G10 mAb, which interacts with an epitope in the center of apoA-I, giving values of ED_{50} between 0.008 and 0.052 μg/mL, compared to 0.5−2.0 μg/mL measured with the other mAbs. The ED_{50} values were

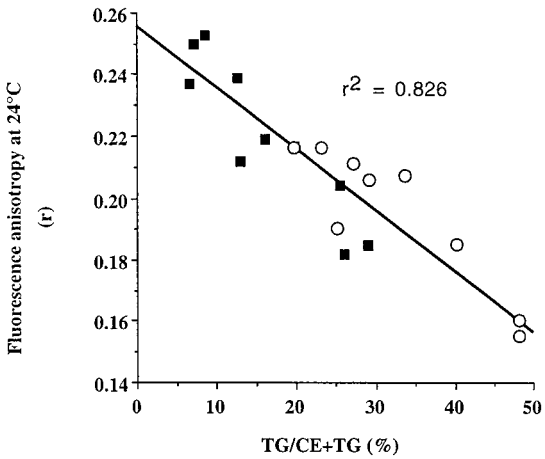

FIGURE 4: Correlation between the triacylglycerol content of the hydrophobic core of TG-rich HDL_2 (○) or r-HDL_2(■) and the fluorescence anisotropy (r) at 24 °C. Lipid dynamics were obtained by fluorescence polarization as described in Table 3.

significantly different between HDL_2 and HDL_3 (from $p < 0.05$ to $p < 0.005$), and in most cases, small-sized HDL_3 displayed a higher immunoreactivity than larger HDL_2 in agreement with previous observations (*22*). We observed increased immunoreactivities of TG-rich HDL_2 as compared to native HDL_2 for most epitopes studied (3G10, 5F6, A03, A05, and A16, $p < 0.02$). When remnant-HDL_2 and TG-rich HDL_2 were compared, most mAbs reacted identically with the two particles. However, a significant change was recorded for the 2G11 epitope, which was less reactive in remnant-HDL_2 than in its parent particle ($p < 0.05$). The

Table 4: Immunoreactivity of HDL$_3$, HDL$_2$, TG-HDL$_2$, and Remnant-HDL$_2$ toward Monoclonal Antibodies, as Measured by Competitive RIA[a]

mAb	HDL$_3$	HDL$_2$	TG-HDL$_2$	r-HDL$_2$
2G11	1.47 ± 0.72	4.13 ± 2.58	3.86 ± 1.15	6.50 ± 2.80
3G10	0.008 ± 0.004	0.052 ± 0.010	0.033 ± 0.010	0.034 ± 0.010
5F6	0.37 ± 0.01	4.97 ± 1.70	1.27 ± 0.31	1.34 ± 0.24
A03	0.54 ± 0.09	1.18 ± 0.31	0.69 ± 0.08	0.81 ± 0.04
A05	0.50 ± 0.25	3.41 ± 0.57	1.58 ± 0.48	1.59 ± 0.41
A16	0.42 ± 0.20	3.02 ± 0.58	1.73 ± 0.62	1.69 ± 0.68
A51	2.11 ± 0.64	0.61 ± 0.30	0.57 ± 0.08	0.96 ± 0.43

[a] Apo-HDL, 2 μg/mL, was coated and was used as a solid-phase antigen. Serial dilutions of the particles were assayed as competing antigens against the different mAbs, diluted as described in Experimental Procedures. Values are the means ±SD of the corresponding ED$_{50}$ from 6 independent experiments. The ED$_{50}$ values were significantly different between HDL$_2$ and HDL$_3$ for all mAbs ($p < 0.05$). Values were significantly different between HDL$_2$ and TG-rich HDL$_2$ for 3G10, 5F6, A03, A05, and A16 ($p < 0.02$). The ED$_{50}$ for 2G11 was significantly different between r-HDL$_2$ and TG-rich HDL$_2$ ($p < 0.05$. All values between r-HDL$_2$ and HDL$_3$ were significant at the $p < 0.02$ level.

2G11 mAb recognizes a discontinuous epitope encompassing severals segments in the N-terminus of apoA-I.

DISCUSSION

High-density lipoproteins (HDL) undergo constant remodeling in the vascular compartment, due to the intricate effects of lipolytic enzymes and lipid transfer proteins. Particularly, the continuous action of lecithin−cholesterol acyl transferase (LCAT) generates spherical HDL of increasing size (*2*). The further activity of cholesteryl ester transfert protein (CETP) leads to the formation of triglyceride-rich, large HDL particles (triglyceride-rich HDL$_2$), containing up to 30% triacylglycerol in their lipid core composition (*4*, *7*). Under physiological conditions, such modifications are observed during post-prandial lipemia (*7*, *9*). Moreover, the triglyceride content of HDL$_2$ among individuals displays a high degree of variation, as much as 8-fold, and is closely associated with the magnitude of post-prandial lipemia (*8*). Several studies have suggested that the enrichment of HDL$_2$ with TG and their further hydrolysis by vascular-bound lipases would be key events in HDL particle interconversion (*4*, *7*, *28*). More recently, we have demonstrated that hepatic lipase acting on TG-rich HDL$_2$ induces the splitting of one substrate particle into two product particles, preβ_1-HDL on one hand, the early HDL acceptor of cellular cholesterol, and remnant HDL$_2$ on the other hand (*1*). In this study, we have been able to isolate both types of particles, as generated through the action of hepatic lipase in vitro, and then to characterize them.

The isolated preβ_1-HDL obtained display a chemical composition very comparable to that of the preβ_1-HDL isolated from the follicular fluid, a model of extravascular compartment, except for a lower content in phospholipids (*16*). Follicular fluid lipoproteins, which only contain HDL, most likely originate from plasma, by filtration through the follicular barrier. This similitude between the preβ_1-HDL formed in vitro and those isolated from follicular fluid argues in favor of a physiological role for hepatic lipase in the generation of preβ_1-HDL (*16*). The presence in these particles of a hydrophobic core of apolar lipids confirmed our earlier studies (*16*) and studies by Wong et al. (*14*) on the preβ_1-HDL isolated from dog plasma and lymph. The preβ_1-HDL contain 1 to 2 molecules of apoA-I reflecting some heterogeneity among these particles. Since the remnant-HDL$_2$ have lost one apoAI molecule, on average, it seems likely that preβ_1-HDL containing a single apoA-I are first generated, and that particles fusion may occasionally occur leading to complexes containing 2 molecules of apoA-I.

The remnant-HDL$_2$ generated through lipolysis are clearly different from the substrate particles. Compared to TG-rich HDL$_2$, remnant particles have lost one apoA-I molecule, 60% of triacylglycerols, and 15% of phospholipids, but have retained their content in free/esterified cholesterol. These modifications are accompanied by a decrease in particle size and mass (274 kDa for the remnant-HDL$_2$ versus 327 kDa for TG-rich HDL$_2$). Remnant-HDL$_2$ are also different from HDL$_3$ in terms of size, molecular composition (*27*), and apoA-I immunoreactivity toward all mAbs studied ($p < 0.02$). It is generally accepted that hepatic lipase triggers the conversion of HDL$_2$ into HDL$_3$, the two major subfractions encountered in human plasma. Our data do not support this view and rather suggest that remnant-HDL$_2$ is a distinct subpopulation whose metabolic fate has still to be determined.

Diacylglycerols (DG) were found in TG-rich HDL$_2$, in agreement with our recent observations on HDL$_2$ and HDL$_3$ (*27*), although the DG/TG ratio was lower in TG-rich HDL$_2$ than in unmodified HDL$_2$. Surprisingly, the amount of DG was found unchanged in remnant-HDL$_2$. Diacylglycerols are a very good substrate for hepatic lipase, as recently demonstrated by Coffil et al. (*29*), using reconstituted HDL. On the other hand, DG are an intermediate product of TG lipolysis. Their constant level in HDL particles along the lipolysis process suggests some equilibrium between the generation of DG and their disappearance upon action of hepatic lipase. The exact role of these molecules in the structure of HDL remains to be established.

Monoclonal antibodies against apoA-I are useful tools to follow changes in apolipoprotein conformation, as induced by in vitro modifications (*22*). The TG enrichment of HDL$_2$ induces an increased immunoreactivity of several epitopes, notably of those located in the center of the molecule, a region of densely packed α-helices (3G10, 5F6, A03, A05). The ED$_{50}$ values for these different epitopes are intermediate between those of HDL$_2$ and HDL$_3$. Regarding remnant-HDL$_2$, no change was recorded in the immunoreactivity toward most mAbs. This suggests that there is no major reorganization of apoA-I at the surface of HDL particles due to HL-mediated lipolysis, despite the loss of 1 apoA-I molecule out of 4. The only significant modification in remnant-HDL$_2$ versus TG-rich HDL$_2$, is a decreased immunoreactivity toward the 2G11 mAb. The 2G11 epitope is a complex, discontinuous epitope, like others in the N-terminal end of apoA-I. It interacts with segments mostly located in the two short first α-helices (residues 44−50 and 58−64), at the middle of the neighboring helix (residues 77−83), and around amino acid 94. The 2G11 epitope is highly conformation- and phospholipid-dependent (*22*). In the present case, there was no change in the PL/A-I ratio between TG-rich HDL$_2$ and remnant-HDL$_2$. It is likely that 2G11 immunoreactivity indicates subtle changes in the conformation of the N-terminal region of apoA-I. The relative masking of the 2G11 epitope in remnant-HDL$_2$ might occur as a

consequence of rearrangements of neighboring epitopes, not explored with the available mAbs. Interestingly, the HPLC peptide profiles after a mild treatment by trypsin show different patterns between TG-rich HDL_2 modified or not by hepatic lipase (not shown, Valérie Georgeaud and Karim Guendouzi, work in progress).

By fluorescence polarization and electron spin resonance (*18*), we evidenced a decreased fluidity of remnant-HDL_2 as compared to TG-rich HDL_2. If one compares the fluorescence anisotropy and the degree of order of TG-rich HDL_2, 0.208 and 0.695, to those of unmodified HDL_3, 0.240 and 0.740, as reported in ref *18*, it is clear that TG-rich HDL_2 display an increased fluidity of the envelope lipids. This might be due to size differences or rather to the enrichment of the particle core with triacyglycerols. Indeed, following TG hydrolysis both parameters are increased, and we observed a negative relationship between fluorescence anisotropy and the contribution of TG to the lipid core (Figure 4). Hence, triacylglycerols are likely to increase HDL fluidity. A previous study using the same approach (*18*) demonstrated that phosphatidylcholine hydrolysis also decreased fluidity. Thus, because of the loss of triacylglycerols and of phospholipids in remnant-HDL_2, apoA-I is probably more condensed in those particles than in the substrate TG-rich HDL_2. This is concordant with earlier reports (*30*, *31*), which described the effects of cholesteryl ester and triacylglycerol molecules in reconstituted HDL on the physical properties of apoA-I which, in TG-rich reconstituted HDL, is less stable than in CE-rich particles. Thus, after treatment by hepatic lipase, the dynamic properties of HDL are completely modified.

Preβ_1-HDL and remnant-HDL_2 are formed during hydrolysis by hepatic lipase, both in vitro and in recycling liver perfusions. In the latter case, preβ_1-HDL accumulate in the perfusate for up to 1 h while remnant particles progressively disappear during the same period of time (*1*). However, remnant-HDL_2 produced in vitro were found to be stable. Thus, remnant-HDL_2 might be very actively taken up by liver cells and would thus represent a privileged particle, as regards the mechanisms of interactions with hepatocytes. If this was verified, it would suggest some collaborative mechanisms between hepatic lipase and putative HDL receptors. Studies have been conducted in our laboratory to test the different aspects of these cellular interactions of remnant-HDL_2 compared to untreated HDL subfractions (*32*). The physicochemical characterization of those remnant-HDL_2 presented in this manuscript will open up new perspectives regarding the metabolic fate of those new HDL particles.

REFERENCES

1. Barrans, A., Collet, X., Barbaras, R., Jaspard, B., Manent, J., Vieu, C., Chap, H., and Perret, B. (1994) *J. Biol. Chem. 269*, 11572−11577.
2. Glomset, J. A. (1968) *J. Lipid Res. 9*, 155−167.
3. Tall, A. R. (1993) *J. Lipid Res. 34*, 1255−2174.
4. Deckelbaum, R. J., Eisenberg, S., Oschry, Y., Granot, E., Sharon, I., and Bengtsson-Olivecrona, G. (1986) *J. Biol. Chem. 261*, 5201−5208.
5. Perret, B. P., Chollet, F., Durand, S., Simard, G., Chap, H., and Douste-Blazy, L. (1987) *Eur. J. Biochem. 162*, 279−286.
6. Brouillette, C. G., and Anantharamaiah, G. M. (1995) *Biochim. Biophys. Acta 1256*, 103−129.
7. Patsch, J. R., Prasad, S., Gotto, A. M., and Bengtsson-Olivecrona, G. (1984) *J. Clin. Invest. 74*, 2017−2023.
8. Patsch, J. R., Prasad, S., Gotto, A. M., and Patsch, W. (1987) *J. Clin. Invest. 80*, 341−347.
9. Murakami, T., Michelagnoli, S., Longhi, R., Gianfranceschi, G., Pazzuconi, F., Calabresi, L., Sirtori, C. R., and Franceschini, G. (1995) *Arterioscler. Thromb. Vasc. Biol. 15*, 1819−1828.
10. Azema, C., Marques-Vidal, P., Lespine, A., Simard, G., Chap, H., and Perret, B. (1990) *Biochim. Biophys. Acta 1046*, 73−80.
11. Castro, G. R., and Fielding, C. J. (1988) *Biochemistry 27*, 25−29.
12. Lefevre, M., Sloop, C. H., and Roheim, P. S. (1988) *J. Lipid Res. 29*, 1139−1148.
13. Ishida, Y., Frolich, J., and Fielding, C. J. (1987) *J. Lipid Res. 28*, 778−785.
14. Wong, L., Sivok, B., Kurucz, E., Sloop, C. H., Roheim, P. S., and Asztalos, B. (1995) *Arterioscler. Thromb. Vasc. Biol. 15*, 1875−1881.
15. Barrans, A., Jaspard, B., Barbaras, R., Chap, H., Perret, B., and Collet, X. (1996) *Biochim. Biophys. Acta 1300*, 73−85.
16. Jaspard, B., Collet, X., Barbaras, R., Manent, J., Vieu, C., Parinaud, J., Chap, H., and Perret, B. (1996) *Biochemistry 35*, 1352−1357.
17. Collet, X., Perret, B., Simard, G., Vieu, C., and Douste-Blazy, L. (1990) *Biochim. Biophys. Acta 1043*, 301−310.
18. Lottin, H., Motta, C., and Simard, G. (1996) *Biochim. Biophys. Acta 1301*, 127−132.
19. Dachet, C., Motta, C., Neufcour, D., and Jacotot, B. (1990) *Biochim. Biophys. Acta 1046*, 64−72.
20. Bonnefont-Rousselot, D., Motta, C., Khalil, A. O., Sola, R., La Ville, A. E., Delattre, J., and Gardes-Albert, M. (1995) *Biochim. Biophys. Acta 1255*, 23−30.
21. Marcel, Y. L., Jewer, D., Vezina, C., Milthorp, P., and Weech, P. K. (1987) *J. Lipid. Res. 28*, 768−777.
22. Collet, X., Perret, B., Simard, G., Raffaï, E., and Marcel, Y. L. (1991) *J. Biol. Chem. 266*, 9145−9152.
23. Nilsson-Ehle, P., and Eckman, R. (1977) *Artery 3*, 194−209.
24. Roschlau, P., Bernt, E., and Gruber, W. (1974) *Z. Klin. Chem. Klin. Biochem. 12*, 403−407.
25. Böttcher, C. J. F., Van Gent, C. M., and Pries, C. (1961) *Anal. Chim. Acta 24*, 203−204.
26. Skipski, V. P., Peterson, F. F., and Barclay, M. (1964) *Biochem. J. 90*, 374−379.
27. Vieu, C., Jaspard, B., Barbaras, R., Manent, J., Chap, H., Perret, B., and Collet, X. (1996) *J. Lipid Res. 37*, 1153−1161.
28. Newnham, H. H., and Barter, P. J. (1990) *Biochim. Biophys. Acta 1044*, 57−64.
29. Coffil, C. R., Ramsamy, T. A., Hutt, D. M., Schultz, J. R., and Sparks, D. L. (1997) *J. Lipid. Res. 38*, 2224−2231.
30. Sparks, D. L., Davidson, W. S., Lund-Katz, S., and Phillips, M. C. (1993) *J. Biol. Chem. 268*, 23250−23257.
31. Sparks, D. L., Davidson, W. S., Lund-Katz, S., and Phillips, M. C. (1995) *J. Biol. Chem 270*, 26910−26917.
32. Guendouzi, K., Collet, X., Perret, B. P., Chap, H., and Barbaras, R. (1998) *Biochemistry 37*, 14974−14980.

BI9815086